
http://www.diva-portal.org

Postprint

This is the accepted version of a paper presented at *Micromechanics and Microsystems Europe Workshop (MME 2018, Aug. 26-29, Smolenice, Slovakia)*.

Citation for the original published paper:

Svensson, K., Södergren, S., Andersson, M., Klintberg, L., Hjort, K. (2018)
High-pressure microfluidic electrochemical and image analysis dual detection for HPLC
In: (pp. 113-119).

N.B. When citing this work, cite the original published paper.

Permanent link to this version:
http://urn.kb.se/resolve?urn=urn:nbn:se:uu:diva-367300

High-pressure microfluidic electrochemical and image analysis dual detection for HPLC

Karolina Svensson, Simon Södergren, Martin Andersson, Lena Klintberg, Klas Hjort

Uppsala University, Centre of Natural Hazards and Disaster Science, CNDS, and Department of Engineering Sciences, Division of Microsystem Technology, Box 534, SE-75121 Uppsala, Sweden

karolina.svensson@angstrom.uu.se, simon.sodergren@angstrom.uu.se and klas.hjort@angstrom.uu.se

Abstract. High-performance liquid chromatography (HPLC) is often set as the lab-based golden standard. For point-of-care and point-of-site applications, making HPLC portable, easy to use and low cost, is very desirable. To reach lower costs, one important task is the development of suitable detectors. Because of the potential for low cost and high performance, a dual-detection microfluidic chip with an electrochemical detector (ECD) and optical access for image analysis was evaluated at high pressure, downstream an HPLC column. For the image analysis, a camera and near-UV-light was used to extract absorption data. To validate the response, a spectrometer was coupled downstream the chip. The results of the three different detectors were comparable, with the camera providing similar absorbance-time chromatograms as the spectrometer. However, the ECD registered only peaks from one of two analytes. To conclude, this experimental setup has potential to provide better understanding of the capability for microfluidic HPLC systems.

1. Introduction

High-performance liquid chromatography (HPLC) is separating, at high pressure, a mixture of smaller amounts of analytes to establish the presence or relative proportions of them. It provides good detection for many diagnostic, environmental, and process monitoring applications. There are good reasons in integrating HPLC in high-pressure tolerant microfluidic systems with mass spectroscopy [1][2]. Also, if HPLC was easier to use, and the cost could be reduced, point-of-care and point-of-site could provide many important applications, hence decreasing the need to send samples to central analytical laboratories.

One important feature to reach lower costs is the detection of the separated analytes. The often used multi-wavelength UV-VIS detectors have a disadvantage in high cost. Electrochemical detection (ECD) is an alternative and very sensitive technique for oxidizable and reducible compounds in HPLC [3]. Recently, a way to integrate thin film sensors into high-pressure tolerant microfluidic chips has been demonstrated [4]. The developed procedure can also be used to make a pressure tolerant microfluidic ECD, with potential for low costs.

Pluangklang *et al.* showed that dual-detection systems may provide higher selectivity and specificity than what one detector could provide alone [5]. To forward this work to HPLC systems using compressible liquids, like gas expanded liquids, it would be good if such a chip can handle high pressure.

ThermoFisher Scientific has commercialized an ECD in HPLC, *e.g.* UltiMate™ 3000 ECD-3000RS, and claims that for certain analytes, this ECD offers direct measurement to femtogram levels in limited sample volumes and with minimal preparation [6]. This could potentially make ECD suitable for point-of-care self-tests where only limited blood volumes by finger-pricking may be used.

In this paper, a high-pressure microfluidic dual-detection microfluidic chip, using ECD together with a low-cost camera that reaches down to near-UV in combination with image analysis, is demonstrated downstream an HPLC column. This gives better understanding and possibility to optimize the microfluidic system since the system can show the plug shape in more detail as well as provide a chance for dual-detection. The aim is to provide a better understanding of the capability of the system and its potential in providing useful low cost detection in microfluidic high-pressure chromatographic systems.

2. Materials and method

2.1. Chip Design and Assembly

A microfluidic chip is used for optical and electrochemical readout of the output from the HPLC column and a spectrometer is coupled in series with the chip to validate the results.

For the electrochemical sensor, thin film electrode arrays are embedded in trenches on a 1.1 mm thick borosilicate wafer enclosed by bonding another wafer with etched microchannels on top. The electrode material must be compatible with the fabrication method and work as an electrochemical detector. Consequently, Pt was chosen because it is highly corrosion resistant and is commonly used as the electrode material in electrochemistry. 110 nm Pt was sputtered on 30 nm Ta that forms an adhesion layer in-between Pt and the glass wafer.

The straight microfluidic channel has an approximately semi-circular cross-section with 360 µm width and 150 µm depth. The channel has openings on opposite sides of the chip, giving access to a chemical inlet and outlet through glass capillaries. A restrictor channel of 60 µm width is positioned at the centre of the channel forming a bridge between the inlet and outlet channels where the electrode array is positioned.

An array of six electrodes were designed with different sizes. Three of these electrodes were used, one large counter electrode (CE), one micro working electrode (WE) and one pseudo reference electrode (RE). In this paper, a 1000 µm wide electrode was used as CE, the smallest 5 µm electrode was used as WE and the 10 µm electrode was used as the RE, Figure 1a and b.

A camera was positioned above the chip to capture an area before the restrictor containing both the channel and a blank area outside the channel, Figure 1c. The chip fabrication method used has been described elsewhere [4].

To be able to flow fluid to the chip, glass capillaries (outer Ø105 µm, inner Ø40 µm) was inserted into the inlet and outlet channels and then glued at the interface. To connect the capillaries to the rest of the HPLC system, tubes (PEEK 1/16, inner Ø178 µm, Upchurch Scientific) were glued to the capillaries. The assembled chip was mounted on a printed circuit board (PCB) that was used to gain electrical access to the electrodes. The transparent chip material and a hole in the PCB enabled optical access to the channel. To make the assembled chip more robust, the tubes were mechanically strain relieved.

2.2. Experimental setup

To evaluate the microfluidic dual detector, a setup with the following parts was mounted: a high-pressure piston pump (100 DM, ISCO Teledyne), an injection valve (Cheminert valve, VICI), a reversed phase separation column (YMC-triart, C18, inner Ø2 mm, length 100 mm), a potentiostat (Type III, µAUTOLAB), a camera (DFK 33UX174, The Imaging Source), an UV LED array (UV High power LED Chip 370 ± 20 nm) and a spectrometer (Ocean HDX, OceanOptics) that includes a deuterium lamp (DH-2000, OceanOptics), a shutter, and a cuvette (Agilent 1100 flow cell G1315, Agilent Technologies), Figure 1d.

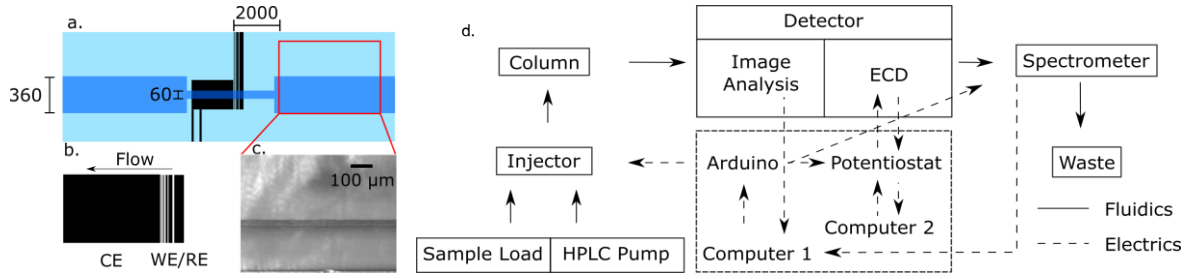

Figure 1. (a) Drawing of the microfluidic detector chip. The electrode array (b) has the following electrode widths in µm (from left to right); 1000, 5, 10, 20, 40, 100. A camera image (c) from the analysis position of the channel. (d) Principal drawing of the microfluidic HPLC dual-detection setup that show the Arduino monitoring and the fluidic pathway from the HPLC pump, through the column and the detectors.

To get access to a simultaneous dual detection, the assembled chip was fixed in a microscope with the camera above and the UV LED array underneath while the potentiostat was connected to the chip. The spectrometer was coupled in series with the chip by an 18 cm PEEK tube (inner Ø178 µm) connected to a 17 cm long thin capillary leading to the cuvette with an optical path length of 1 cm. Optical fibres were fixed on each side of the cuvette and the shutter to the lamp was automatically opened when the sample was injected.

To control the time of the simultaneous detections, Matlab (Matlab R2018a, MathWorks) and an Arduino (Uno, Arduino) was used to monitor the valve injection, the potentiostat, the deuterium lamp shutter and the image acquisition from the camera.

2.3. Chemicals

The mobile phase was prepared by mixing 35% deionized water with 65% acetonitrile (≥99.9%, HiPerSolv Chromanorm, VWR Chemicals) with 1% formic acid (98%, GPR Rectapur, VWR Chemicals). The mobile phase was degassed with ultrasonication for 30 min and filtered (A-703 PEEK frit 0.45 µm, IDEX) two times. The sample solution was prepared by diluting xanthohumol (≥98% Biovision, WVR Chemicals) with ethanol (ethanol Absolute 99.9%, AnalaR Normapur, VWR Chemicals) to a concentration of 5, 10, 50, 250, 500, 750 and 1000 µM.

2.4. Measurements

To determine what flow rates that could be used, a pressure tolerance test was performed. One chip was plugged at the outlet channel while flowing CO_2 with an applied pressure that was increased with steps of 10 bars until fracture.

The evaluation of the microfluidic dual detector was performed with a 10 cm long column. The flow rate of the mobile phase was set to 100 µl/min corresponding to a pressure of 65 bar with an atmospheric back pressure. The potentiostat was set to chronoamperometric mode with the detection voltage +2 V. A 2 µl sample of 750 µM xanthohumol was injected at the same time as the ECD and the image analysis was started, and the shutter was opened.

To gain a more sensitive ECD signal with horizontal baselines, a pulsed amperometric study was made. This study was performed by cycling 4 potential steps during the measurement to keep the working electrode as homogeneous as possible during the experiment. Each cycle starts with the measuring potential at +0.8 V in 0.2 s, then a reactivating step at -2 V in 0.3 s followed by a cleaning step at +0.6 V in 0.03 s and a last reactivating step at -0.1 V in 0.1 s.

To verify the possibilities for quantitative detections, a concentration series of xanthohumol were performed with image analysis and the spectrometer. The concentrations were 5, 10, 50, 250, 500, 750 and 1000 µM and each measurement was done in triplicates.

To investigate if the fabricated ECD could detect xanthohumol, a non-aqueous ECD study was made. This was performed by using chronoamperometric detection while flowing ethanol through the

chip from a pump (PHD 2000 Infusion, Harvard) at 20 µl/min while repeatedly injecting 1000 µM xanthohumol from the injection valve. No column was used during this study. The potential chosen was +0.8 V (vs. pseudo Pt reference) and to obtain a more sensitive signal, tests were made with a shielding self-made Faraday cage.

The simultaneous HPLC dual detection was planned for an aqueous system. Pt based electrochemical detections in aqueous environments is difficult because oxygen adsorption passivates the electrodes. An aqueous ECD study was therefore performed using the experimental setup described in Figure 4. The study was performed by using +0.8 V amperometric detection while flowing the aqueous mobile phase through the chip and injecting xanthohumol with varying concentrations through the column. Measurements were also made with a pre-treatment where the working electrode and the reference electrode was electropolished. The pre-treatment was done by applying +2 V until the baseline was stabilized.

2.5. Data processing

The data that was extracted from the ECD study with ethanol was baseline corrected to make a more accurate comparison between the methods and their parameters. The signal data in the ECD study is smoothed.

An area of 649 µm x 865 µm were covered in the image analysis with a resolution of 480x640 pixels. For absorption analysis, the mean value of 230x640 pixels from the channel where used and 200x640 pixels from the blank area. The absorbance of the analytes was calculated with the definition of absorbance by dividing the mean values of the intensity from the blank area in the image, I_0, with the intensity from the area of the channel, I_1:

$$A = -\log_{10}\frac{I_1}{I_0} \quad (1)$$

The background from the mobile phase was removed by subtracting the values from a fitting of a third order polynomial to the points excluding the peaks. The absorbance profile for the cross section of the channel was evaluated by calculating the mean value of each horizontal pixel row. The value was plotted against the width of the channel and the time to get a 2D mapping of the plug.

The values from the spectrometer measurement at λ=370 and λ=240 nm were extracted and the time for when the shutter opened was subtracted.

To compare concentrations, the area of the background adjusted peaks from the image analysis and the area of the peaks from the spectrometer with λ=370 nm was calculated with the trapezoidal method in Matlab (Matlab R2017a, MathWorks) with integration over time in minutes.

3. Results

The pressure test resulted in a tolerance of 140 bar for the microfluidic chip. The bonded glass around the restrictor channel appeared to be the weakest point.

3.1. Dual detection study

The results from the dual detection study are presented in Figure 2. The ECD detected ethanol but not xanthohumol. Pulsed amperometric detection did not only show a more horizontal baseline than chronoamperometry, it also showed higher sensitivity for ethanol. The ethanol shows the dead time of the system, *i.e.* the time it takes for unretained media to reach the detector. Both the ECD and image analysis detected the start of the ethanol peak at 1.5 min. The peaks obtained with the spectrometer was detected 0.2 min after the dual detectors.

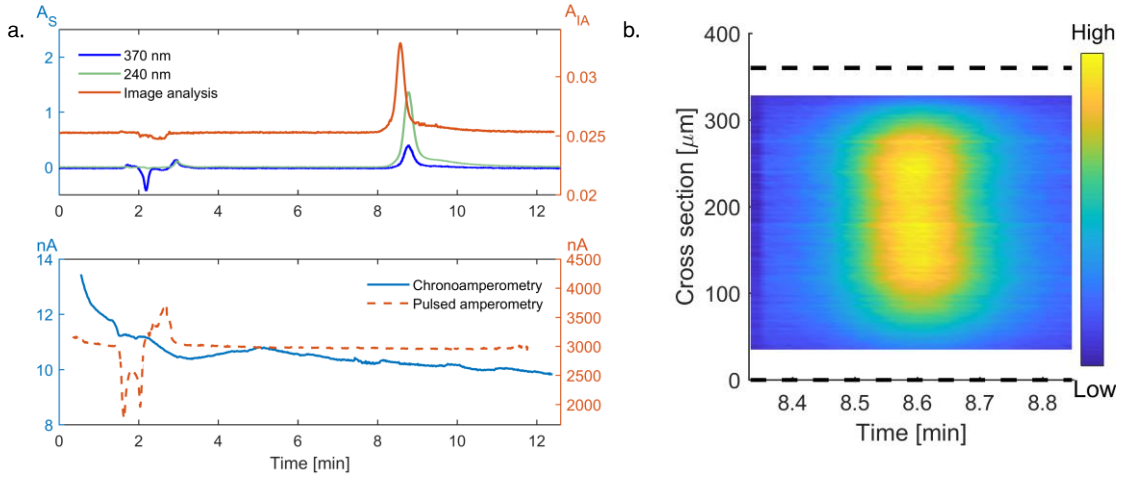

Figure 2. a. (top) Chromatograms with absorbance from the image analysis, $A_{IA,}$ and the spectrometer (at λ = 240 nm and λ = 370 nm), A_S. (bottom) The ECD responses from the simultaneous chronoamperometry and the principal detection using pulsed amperometry. **b.** A 2D image plot of the mean value from the absorption for each pixel row in an image, plotted against the time and the channel position.

The xanthohumol peak displayed tailing, (clearest seen for 370 nm from the spectrometer measurements in Figure 2a) since the signal decreased slowly before reaching the baseline after the peak. With higher flow rates (up to 130 µl/min) this tail became more distinct, while for lower flow rates (down to 50 µl/min) it decreased.

An absorbance gradient over the cross section can be seen in the 2D plot, Figure 2b. The full width of the channel is 360 µm, but the areas closest to the sides were excluded from the figure because of interfering optical phenomena at the side walls. The y-axis shows the cross section of the channel and the x-axis shows the time, corresponding to the chromatogram in Figure 2a.

3.2. Quantitative analysis of the image analysis detector and the spectrometer

The concentration series confirmed that both the image analysis and the spectrometer could be used for quantitative determinations. Both gave a linear relationship between the concentration and the absorption peak area with R^2=0.999, Figure 3. The pooled estimate of the standard deviation was 5.5% and 3.2% for image analysis and spectrometer, respectively. With the equation from the regression lines the concentration of xanthohumol (prepared as 750 µM) in Figure 2a was calculated to 771 µM and 748 µM for the image analysis and spectrometer, respectively.

3.3. ECD study

When doing repeated injections of xanthohumol in ethanol, clear peaks of high resolution were seen, Figure 6. However, the peak height varied even though the baseline was stable and reproducible for each run.

The aqueous ECD study resulted in non-reproducible results due to non-stable baseline and varying signal current during each experimental run. However, when the electropolishing pre-treatment was performed the baseline became more stable and predictable, but xanthohumol was still not possible to detect repeatedly.

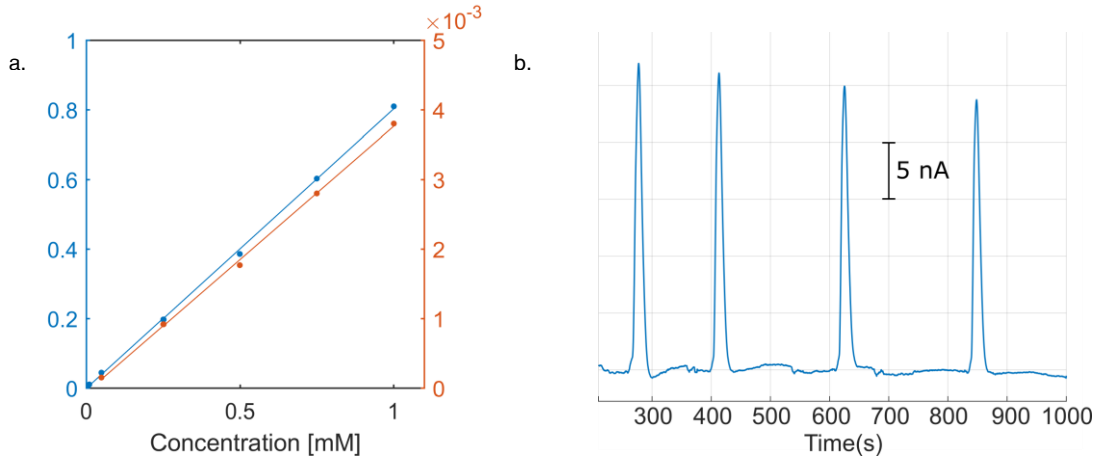

Figure 3. a. Absorbance from the concentration series with a linear regression from the spectrometer to the left (blue) and image analysis to the right (red). **b.** ECD detection of repeatedly injected xanthohumol in ethanol. The plot is baseline corrected and smoothed.

4. Discussion

The dual detection study showed that the dead time for when the ethanol peak started could be detected simultaneously with the image analysis and the ECD detector. Ethanol affects the absorbance and the refractive index of the fluid resulting in altering positive and negative peaks in the absorbance chromatograms. The spectrometer and the image analysis could detect both ethanol and xanthohumol with correlated detection times. The spectrometer peaks appear 0.2 min later, which was expected due to the distance between the chip and the cuvette.

The tailing of the xanthohumol peak in the chromatogram was caused by non-optimal parameters. The tailing increased with higher flow rate and decreased with lower flow rate. This indicates that the diffusion between the stationary phase and the mobile phase wasn't sufficient for the given flow rate of 100 µl/min.

In the 2D plot, the absorbance, and hence the amount of xanthohumol, was higher in the centre of the channel and lower at the sides due to the curved geometry of the wet etched channel resulting in varying optical length. The maximum of the gradient was shifted to one of the sides corresponding to the fact that the capillary outlet was skewed to that side of the channel.

The concentration series resulted in good linearity for both the image analysis and the spectrometer, although the image analysis couldn't detect the two lowest concentrations of 5 and 10 µM. The repeated measurement of the different concentrations reviled that there were a few percent of standard deviation, 5.5% and 3.2% for image analysis and spectrometer, respectively. To reduce this deviation, an internal standard is recommended to normalize the areas of the peaks. To further improve the image analysis, subtracting the signal from blank sample (only mobile phase) should be implemented, and if the signal is averaged over a larger area, the noise is reduced.

The spectrometer is more specific since it can sort out wavelengths while the image analysis gives an absorbance value dependent on all the wavelengths entering from the LEDs. A filter would make it possible to get at signal from a specific wavelength, although only one wavelength could be detected at the time.

Chronoamperometric measurements, Figure 3, result in a declining baseline because of a build-up double layer and a continuous forming of an inert oxide layer on the electrode surface. This inert oxide layer is passivating the electrode, making the baseline current low with a weak signal. In contrast to chronoamperometry, pulsed amperometric measurements result in a baseline current increase, stronger signals and a horizontal baseline due to the continuous cleaning and reactivation of the electrode during the measurements. It is therefore strongly recommended to use pulsed amperometry when using a similar system.

The ECD study with ethanol, Figure 6, showed that xanthohumol gave an electrochemical response but it was difficult to replicate the response. The reason is unknown, but one possible explanation is slow kinetics which means that the oxidation of xanthohumol doesn't have time to occur while the analyte is passing through the electrode. In further studies, it is recommended to try detecting other analytes, reduce the flow rate and use larger electrodes to increase the time the analyte is affected by an electric field. It is also recommended to test other electrode materials such as boron-doped diamond which is an excellent material for electrochemical detections [7].

Based on the pressure test, the chip can be used for high-pressure applications such as Supercritical Fluid Chromatography (SFC). By this, a measurement for SFC-UV/ECD/Image analysis on a microfluidic chip can become possible.

5. Conclusion

To conclude, a dual detection platform for ECD and image analysis was developed with potential to provide better understanding of microfluidic HPLC systems. Although the ECD could detect ethanol, further investigations of other analytes needs to be done before it can be validated as a detector. The image analysis has good chances to be a low-cost alternative to the spectrometer, with capability of quantitative determination.

Acknowledgements

The project was in part founded by the Kamprad Family Foundation. Also, founding for laboratory facilities by Knut and Alice Wallenberg Foundation is acknowledged.

References

[1] D.P. Bishop, L. Blanes, A.B. Wilson, T. Wilbanks, K. Killeen, R. Grimm, R. Wenzel, D. Major, M. Macka, D. Clarke, R. Schmid, N. Cole, and P.A. Doble, "Microfluidic high performance liquid chromatography-chiphyphenation to inductively coupled plasma–mass spectrometry," *J. Chromatogr. A*, vol. 1497, pp. 64–69, 2017.

[2] J. J. Heiland, R. Warias, C. Lotter, P. Fuchs, L. Mauritz, K. Zeitler, S. Ohla, and D. Belder, "On-chip integration of organic synthesis and HPLC/MS analysis for monitoring stereoselective transformations at the micro-scale," *Lab Chip*, vol. 17, pp. 76-81, 2017.

[3] M. B. Hicks, L. Salituro, I. Mangion, W. Schafer, R. Xiang, X. Gong, and C. J. Welch, "Assessment of coulometric array electrochemical detection coupled with HPLC-UV for the absolute quantitation of pharmaceuticals," *Analyst*, vol. 142, pp. 525-536, 2017.

[4] M. Andersson, J. Ek, L. Hedman, F. Johansson, V. Sehlstedt, J. Stocklassa, P. Snögren, V. Pettersson, J. Larsson, O. Vizuete, K. Hjort, and L. Klintberg, "Thin film metal sensors in fusion bonded glass chips for high-pressure microfluidics," *J. Micromech. Microeng*., vol. 27, 015018, 2017.

[5] T. Pluangklang, J.B. Wydallis, D.M. Cate, D. Nacapricha, and C.S. Henry, "A simple microfluidic electrochemical HPLC detector for quantifying Fenton reactivity from welding fumes," *Anal. Methods*, vol. 6, pp. 8180-8186, 2014.

[6] *https://www.thermofisher.com/se/en/home/industrial/chromatography/chromatography-learning-center/liquid-chromatography-information/liquid-chromatography-innovations/electrochemical-detection-liquid-chromatography.html*; *https://www.thermofisher.com/order/catalog/product/5070.0010,* downloaded 2018-06-15

[7] P. Forsberg, E.O. Jorge, L. Nyholm, F. Nikolajeff, and M. Karlsson, "Fabrication of boron doped diamond microband electrodes for electrochemical detection in a microfluidic channel," *Diamond Rel. Mater.*, vol. 20, pp. 1121-1124, 2011.